

Buckling of rectangular plates with mixed edge supports

Y. Xiang[†] and G. H. Su[‡]

Centre for Construction Technology and Research, University of Western Sydney,
Penrith South DC, 1797, Australia

(Received August 29, 2000, Accepted August 26, 2002)

Abstract. This paper presents a domain decomposition method for buckling analysis of rectangular Kirchhoff plates subjected to uniaxial inplane load and with mixed edge support conditions. A plate is decomposed into two rectangular subdomains along the change of the discontinuous support conditions. The automated Ritz method is employed to derive the governing eigenvalue equation for the plate system. Compatibility conditions are imposed for transverse displacement and slope along the interface of the two subdomains by modifying the Ritz trial functions. The resulting Ritz function ensures that the transverse displacement and slope are continuous along the entire interface of the two subdomains. The validity and accuracy of the proposed method are verified with convergence and comparison studies. Buckling results are presented for several selected rectangular plates with various combination of mixed edge support conditions.

Key words: buckling of plates; domain decomposition; Kirchhoff plate; mixed edge support conditions; Ritz method.

1. Introduction

The load carrying capacity of a plate against buckling is one of the most important design aspects in civil, mechanical and aerospace engineering. Numerous studies have been reported in open literature on buckling of plates subjected to various loading and support conditions (Bulson 1970, Column Research Committee of Japan 1971, Reddy and Phan 1985, Xiang *et al.* 1995).

Buckling of plates with mixed boundary conditions has also been investigated by many researchers. Bartlett (1963) conducted a research on the vibration and buckling of a circular plate clamped on part of its boundary and simply supported on the remainder. Hamada *et al.* (1967) studied buckling of simply supported rectangular plates with partially clamped edges. Keer and Stahl (1972) used Fredholm integral equations of the second kind to study buckling and vibration of rectangular plates clamped along the central portion on two opposite edges or clamped partially along one edge, with consideration of stress singularities at the tips of the clamped segment. Sakiyama and Matsuda (1987) applied the numerical integral method for buckling of rectangular Mindlin plates with mixed edge supports. Karamanlidis and Prakash (1989) developed a modified Ritz approach for analysing the buckling and vibration of thick orthotropic plates subjected to mixed

[†] Senior Lecturer

[‡] PhD Candidate

boundary conditions. Using the spline element method, Mizusawa and Leonard (1990) obtained numerical results on buckling and vibration of rectangular and skew plates partially simply supported and partially clamped along two opposite unloaded edges.

Based on the automated Ritz method (Lim and Liew 1993, Xiang *et al.* 1996, Liew *et al.* 1998), a domain decomposition approach is presented in this paper to study buckling of rectangular plates with mixed boundary conditions. The plate is decomposed into two rectangular subdomains along the change of boundary supports. The total potential energy functional of the plate system is derived by summing the total potential energy functional of the two subdomains. Transverse displacement field is approximated with the product of a 2-D complete polynomial and basic functions. The basic functions consist of the product of the boundary equations of a subdomain raised to appropriate powers to ensure automatic satisfaction of the geometric boundary conditions of the subdomain. Continuity conditions at the interface of the two subdomains for transverse displacement and slope are imposed to bridge the two subdomains to form one complete plate. The continuity of the displacement and slope are guaranteed along the entire interface of the two subdomains by modifying the Ritz trial functions. The governing eigenvalue equation for the plate system is derived by minimizing the total potential energy functional of the plate.

Convergence and comparison studies are carried out to verify the validity and accuracy of the method. Buckling results for several selected rectangular plates with different mixed boundary conditions are presented.

2. Mathematical modelling

Consider an isotropic, thin elastic rectangular plate of thickness t , length a , width b , Young's modulus E and Poisson's ratio ν . The plate is subjected to a uniaxial inplane compressive load N in the x direction and may be supported with mixed edge conditions on the edge/edges parallel to the x -axis (see Fig. 1). The objective of the study is to determine the buckling load of the plate.

2.1 Total potential energy functional

To treat the mixed edge support conditions, the plate is partitioned into two subdomains along the change of support conditions. The dimension and coordinate system of each subdomain are shown in Fig. 1. Each subdomain has its own coordinate system with the origin being at the centre of the subdomain. The bending strain energy U and the potential energy of the inplane load V may be expressed as:

$$U = \int_{A^{(1)}} \frac{1}{2} \{ \kappa^{(1)} \}^T [D_k] \{ \kappa^{(1)} \} dA + \int_{A^{(2)}} \frac{1}{2} \{ \kappa^{(2)} \}^T [D_k] \{ \kappa^{(2)} \} dA \quad (1)$$

$$V = -\frac{N}{2} \left[\int_{A^{(1)}} \left(\frac{\partial w^{(1)}}{\partial x_1} \right)^2 dA + \int_{A^{(2)}} \left(\frac{\partial w^{(2)}}{\partial x_2} \right)^2 dA \right] \quad (2)$$

in which the superscripts (1) and (2) refer to subdomains 1 and 2, w is the transverse displacement at the midsurface of the subdomain, A is the area of the subdomain, and $[D_k]$ and $\{ \kappa \}$, the curvature matrix, are given by

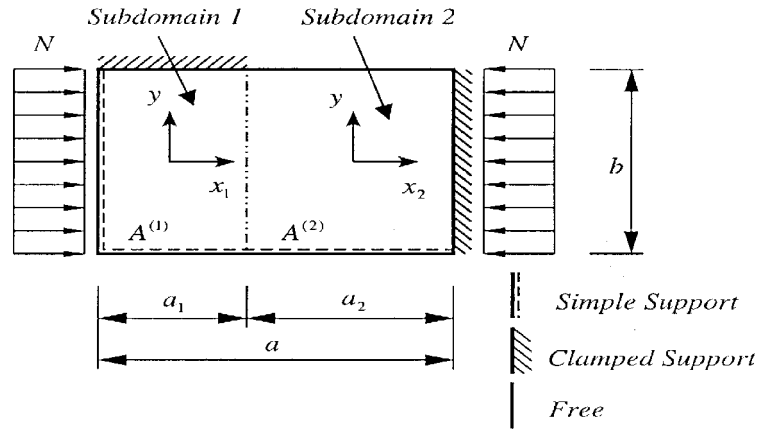


Fig. 1 Geometry and coordinate systems of a rectangular plate with two subdomains

$$[D_k] = \begin{bmatrix} D & D\nu & 0 \\ D\nu & D & 0 \\ 0 & 0 & (1-\nu)D/2 \end{bmatrix} \quad (3)$$

$$\{\kappa^{(1)}\} = \left\{ \frac{\partial^2 w^{(1)}}{\partial x_1^2} \quad \frac{\partial^2 w^{(1)}}{\partial y^2} \quad 2 \frac{\partial^2 w^{(1)}}{\partial x_1 \partial y} \right\}^T \quad (4)$$

$$\{\kappa^{(2)}\} = \left\{ \frac{\partial^2 w^{(2)}}{\partial x_2^2} \quad \frac{\partial^2 w^{(2)}}{\partial y^2} \quad 2 \frac{\partial^2 w^{(2)}}{\partial x_2 \partial y} \right\}^T \quad (5)$$

where $D = Et^3/12(1 - \nu^2)$ is the flexural rigidity of the plate, the symbol $\{ \}$ is used for single column matrices, and the symbol $[]$ is used for rectangular matrices.

The total potential energy functional of the plate is the sum of the bending strain energy U and the potential energy of the inplane load V

$$\Pi = U + V \quad (6)$$

2.2 Governing eigenvalue equation

For simplicity and convenience, the nondimensionalised coordinate systems in the two subdomains, as shown in Fig. 2, are introduced. The origins of the coordinate systems are set at the centres of the subdomains. The following coordinate transformation equations are employed:

$$\xi = \frac{2x_1}{a_1}; \quad \eta = \frac{2y}{b}; \quad r = \frac{2x_2}{a_2} \quad (7, 8, 9)$$

where a_1 and a_2 are the lengths of subdomains 1 and 2 (see Fig. 1), respectively.

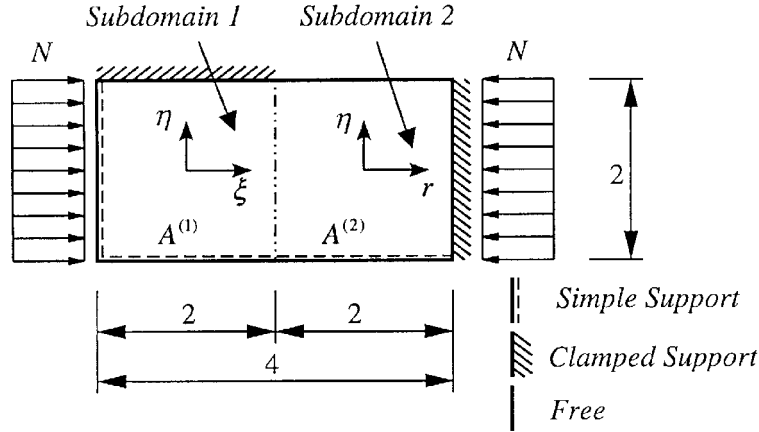


Fig. 2 Geometry and non-dimensionalised coordinate systems of a rectangular plate with two subdomains

Using the automated Ritz method (Lim and Liew 1993, Xiang *et al.* 1996, Liew *et al.* 1998), the transverse displacements for subdomains 1 and 2 can be parameterized as:

$$w^{(1)}(\xi, \eta) = B^{(1)}(\xi)H^{(1)}(\eta) \sum_{i=1}^m a_i \Phi_i(\xi, \eta) = B^{(1)}(\xi)H^{(1)}(\eta) \{\Phi(\xi, \eta)\}_{1 \times m}^T \{a\}_{m \times 1} \quad (10)$$

$$w^{(2)}(r, \eta) = B^{(2)}(r)H^{(2)}(\eta) \sum_{i=1}^n b_i \Gamma_i(r, \eta) = B^{(2)}(r)H^{(2)}(\eta) \{\Gamma(r, \eta)\}_{1 \times n}^T \{b\}_{n \times 1} \quad (11)$$

where the subscript associated with a matrix denotes the matrix dimension (number of rows and number of columns), $\{\Phi(\xi, \eta)\}_{m \times 1}$ and $\{\Gamma(r, \eta)\}_{n \times 1}$ are column matrices containing 2-D complete polynomial of m and n terms for subdomains 1 and 2, respectively, $\{a\}_{m \times 1}$ and $\{b\}_{n \times 1}$ are column matrices of the unknown Ritz coefficients, $B^{(1)}(\xi)$ and $H^{(1)}(\eta)$ are basic functions for subdomain 1, and $B^{(2)}(r)$ and $H^{(2)}(\eta)$ are basic functions for subdomain 2. The number of terms, m and n , of the 2-D complete polynomials are governed by the degrees of the polynomial $p^{(1)}$ and $p^{(2)}$ as follows

$$m = \frac{(p^{(1)} + 1)(p^{(1)} + 2)}{2} \quad (12)$$

$$n = \frac{(p^{(2)} + 1)(p^{(2)} + 2)}{2} \quad (13)$$

The basic functions for subdomains 1 and 2 are the key components in the Ritz trial functions to ensure that the trial functions satisfy the geometric boundary conditions of the two subdomains automatically (Xiang *et al.* 1996). The basic functions consist of the products of the subdomain edge equations raised to appropriate powers:

$$B^{(1)}(\xi) = (\xi + 1)^{\Omega_1} \quad (14)$$

$$H^{(1)}(\eta) = (\eta + 1)^{\Omega_2}(\eta - 1)^{\Omega_3} \tag{15}$$

$$B^{(2)}(r) = (r + 1)^{\Omega_4} \tag{16}$$

$$H^{(2)}(\eta) = (\eta + 1)^{\Omega_5}(\eta - 1)^{\Omega_6} \tag{17}$$

where $\Omega_i, i = 1, 2, \dots, 6$, takes the following values:

$$\Omega_i = 0, \text{ if the } i\text{-th edge is free} \tag{18}$$

$$\Omega_i = 1, \text{ if the } i\text{-th edge is simply supported} \tag{19}$$

$$\Omega_i = 2, \text{ if the } i\text{-th edge is clamped} \tag{20}$$

Note that the Ritz trial functions (Eqs. 10 and 11) satisfy the geometric boundary conditions of the two subdomains through the basic functions. The compatibility conditions along the interface of the two subdomains, however, have not been considered.

For buckling analysis of plates, the C^1 continuity (deflection and slope) needs to be enforced along the interface of the two subdomains, i.e.,

$$w^{(1)}(\xi_0, \eta) = w^{(2)}(r_0, \eta) \tag{21}$$

$$\frac{2}{a_1} \frac{\partial w^{(1)}(\xi_0, y)}{\partial \xi} = \frac{2}{a_2} \frac{\partial w^{(2)}(r_0, y)}{\partial r} \tag{22}$$

in which $\xi_0 = 1$ and $r_0 = -1$ are the coordinates of the interface on the two subdomains. Note that ξ_0 and r_0 are substituted into Eq. (22) after the differentiation is carried out.

The Ritz trial function for subdomain 1, $w^{(1)}$, can be incorporated into the trial function for subdomain 2, $w^{(2)}$, through the compatibility conditions (Eqs. 21 and 22). While the expression for the trial function $w^{(1)}$ remains unchanged, the trial function for subdomain 2, $w^{(2)}$, can be modified by manipulating the compatibility conditions at the interface of the subdomains as follows

$$w^{(2)}(r, \eta) = \{\Psi_a(r, \eta)\}_{1 \times m}^T \{a\}_{m \times 1} + \{\Psi_b(r, \eta)\}_{1 \times (n-2)}^T \{b\}_{(n-2) \times 1} \tag{23}$$

in which

$$\begin{aligned} \{\Psi_a(r, \eta)\}_{1 \times m}^T &= \frac{a_1}{2} f_1 \{\Phi(\xi_0, \eta)\}_{1 \times m}^T + \frac{a_2}{2} (r - r_0) f_2 \{\Phi(\xi_0, \eta)\}_{1 \times m}^T \\ &\quad + \frac{a_2}{2} (r - r_0) f_1 \frac{\partial \{\Phi(\xi_0, \eta)\}_{1 \times m}^T}{\partial \xi} \end{aligned} \tag{24}$$

$$\begin{aligned} \{\Psi_b(r, \eta)\}_{1 \times (n-2)}^T &= B^{(2)}(r) H^{(2)}(\eta) \left(\{\Gamma(r, \eta)\}_{1 \times (n-2)}^T \right. \\ &\quad \left. - (r - r_0) \frac{\partial \{\Gamma(r_0, \eta)\}_{1 \times (n-2)}^T}{\partial r} - \{\Gamma(r_0, \eta)\}_{1 \times (n-2)}^T \right) \end{aligned} \tag{25}$$

$$\{b\}_{(n-2) \times 1} = \begin{Bmatrix} b_3 \\ b_4 \\ \vdots \\ b_n \end{Bmatrix} \tag{26}$$

$$f_1 = \frac{2B^{(1)}(\xi_0)}{a_1 B^{(2)}(r_0)} H^{(1)}(\eta) B^{(2)}(r) \tag{27}$$

$$f_2 = 2 \left(\frac{a_2 \frac{\partial B^{(1)}(\xi_0)}{\partial \xi} B^{(2)}(r_0) - a_1 B^{(1)}(\xi_0) \frac{\partial B^{(2)}(r_0)}{\partial r}}{a_1 a_2 (B^{(2)}(r_0))^2} \right) H^{(1)}(\eta) B^{(2)}(r) \tag{28}$$

The Ritz trial function for subdomain 2 (Eq. 23) has the following characteristics: (1) terms associated with b_1 and b_2 in $w^{(2)}$ have been replaced with terms from the trial function for subdomain 1, $w^{(1)}$. The compatibility conditions along the entire interface of the two subdomains are enforced to have C^1 continuity; (2) the form of polynomial is retained in $w^{(2)}$. Functions f_1 and f_2 in Eqs. (27) and (28) seem to be fraction. Nevertheless, the denominators in f_1 and f_2 are constants; and (3) matrix $\{\Psi_b\}_{1 \times (n-2)}^T$ in Eq. (23), which associated with the unknown coefficients $\{b\}_{(n-2) \times 1}$, has considerable number of zero entries. This damages the completeness of the polynomial, in turn, has adverse effect on the convergence of buckling load.

It is necessary to overcome the defect in matrix $\{\Psi_b\}_{1 \times (n-2)}^T$ in which a large amount of zero entries exists. Since this term needs to vanish at the interface of the two subdomains to satisfy the compatibility conditions, the following expression, which contains a 2-D complete polynomial but vanish itself at the interface, is adopted as a replacement for the original matrix $\{\Psi_b\}_{1 \times (n-2)}^T$ in Eq. (23):

$$\{\Psi_b(r, \eta)\}_{1 \times n}^T = (r - r_0)^2 B^{(2)}(r) H^{(2)}(\eta) \{\Gamma(r, \eta)\}_{1 \times n}^T \tag{29}$$

Accordingly the trial function for $w^{(2)}$ is changed as:

$$w^{(2)}(r, \eta) = \{\Psi^{(2)}(r, \eta)\}_{1 \times (m+n)}^T \{c\}_{(m+n) \times 1} \tag{30}$$

in which

$$\{\Psi^{(2)}(r, \eta)\}_{1 \times (m+n)}^T = \{\{\Psi_a(r, \eta)\}_{1 \times m}^T \{\Psi_b(r, \eta)\}_{1 \times n}^T\} \tag{31}$$

$$\{c\}_{(m+n) \times 1} = \begin{Bmatrix} \{a\}_{m \times 1} \\ \{b\}_{n \times 1} \end{Bmatrix} \tag{32}$$

The trial function for subdomain 1 can also be expressed as

$$w^{(1)}(\xi, \eta) = \{\Psi^{(1)}(\xi, \eta)\}_{1 \times (m+n)}^T \{c\}_{(m+n) \times 1} \tag{33}$$

where

$$\{\Psi^{(1)}(\xi, \eta)\}_{1 \times (m+n)}^T = \{\{\Phi_a(\xi, \eta)\}_{1 \times m}^T \quad \{0\}_{1 \times n}^T\} \quad (34)$$

$$\{\Phi_a(\xi, \eta)\}_{1 \times m}^T = B^{(1)}(\xi)H^{(1)}(\eta)\{\Phi(\xi, \eta)\}_{1 \times m}^T \quad (35)$$

It should be noted that the trial functions defined in Eqs. (30) and (33) only satisfy the geometric interface conditions between subdomains, i.e., it ensures the continuity of the transverse displacement w and the slope $\partial w / \partial x$ along the interface of the subdomains.

Substituting Eqs. (33) and (30) into Eq. (6) and minimising the total potential energy functional with respect to the unknown Ritz coefficients leads to the following governing eigenvalue equation for buckling of the plate system:

$$([K]_{(m+n) \times (m+n)} - N[G]_{(m+n) \times (m+n)})\{c\}_{(m+n) \times 1} = \{0\}_{(m+n) \times 1} \quad (36)$$

where $[K]_{(m+n) \times (m+n)}$ and $[G]_{(m+n) \times (m+n)}$ are the stiffness and geometric matrices of the plate which are derived as follows

$$[K]_{(m+n) \times (m+n)} = [K^{(1)}]_{(m+n) \times (m+n)} + [K^{(2)}]_{(m+n) \times (m+n)} \quad (37)$$

$$[G]_{(m+n) \times (m+n)} = [G^{(1)}]_{(m+n) \times (m+n)} + [G^{(2)}]_{(m+n) \times (m+n)} \quad (38)$$

$$[K^{(1)}]_{(m+n) \times (m+n)} = \frac{a_1 b}{4} \int_{-1}^1 \int_{-1}^1 [\chi^{(1)}]^T [D_k] [\chi^{(1)}] d\xi d\eta \quad (39)$$

$$[G^{(1)}]_{(m+n) \times (m+n)} = \frac{b}{a_1} \int_{-1}^1 \int_{-1}^1 \frac{\partial \{\Psi^{(1)}(\xi, \eta)\}_{(m+n) \times 1}}{\partial \xi} \frac{\partial \{\Psi^{(1)}(\xi, \eta)\}_{1 \times (m+n)}^T}{\partial \xi} d\xi d\eta \quad (40)$$

$$[K^{(2)}]_{(m+n) \times (m+n)} = \frac{a_2 b}{4} \int_{-1}^1 \int_{-1}^1 [\chi^{(2)}]^T [D_k] [\chi^{(2)}] dr d\eta \quad (41)$$

$$[G^{(2)}]_{(m+n) \times (m+n)} = \frac{b}{a_2} \int_{-1}^1 \int_{-1}^1 \frac{\partial \{\Psi^{(2)}(r, \eta)\}_{(m+n) \times 1}}{\partial r} \frac{\partial \{\Psi^{(2)}(r, \eta)\}_{(m+n) \times 1}^T}{\partial r} dr d\eta \quad (42)$$

$$[\chi^{(1)}] = \begin{bmatrix} \left(\frac{2}{a_1}\right)^2 \frac{\partial^2 \{\Psi^{(1)}(\xi, \eta)\}_{1 \times (m+n)}^T}{\partial \xi^2} \\ \left(\frac{2}{b}\right)^2 \frac{\partial^2 \{\Psi^{(1)}(\xi, \eta)\}_{1 \times (m+n)}^T}{\partial \eta^2} \\ \left(\frac{8}{a_1 b}\right) \frac{\partial^2 \{\Psi^{(1)}(\xi, \eta)\}_{1 \times (m+n)}^T}{\partial \xi \partial \eta} \end{bmatrix} \quad (43)$$

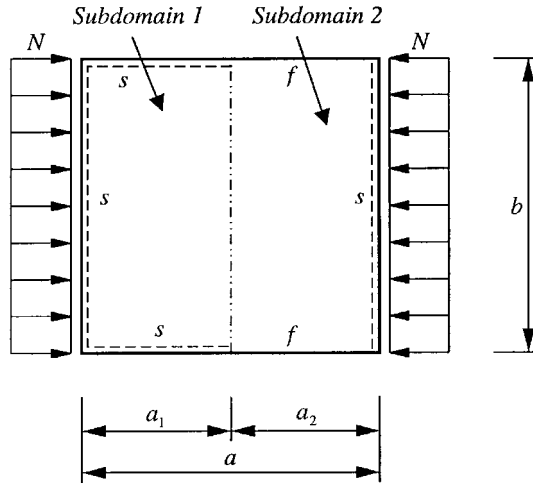


Fig. 3 A square plate subjected to uniaxial in-plane load and having mixed edge support conditions (ss-sff plate)

$$[\chi^{(2)}] = \begin{bmatrix} \left(\frac{2}{a_2}\right)^2 \frac{\partial^2 \{\Psi^{(2)}(r, \eta)\}_{1 \times (m+n)}^T}{\partial r^2} \\ \left(\frac{2}{b}\right)^2 \frac{\partial^2 \{\Psi^{(2)}(r, \eta)\}_{1 \times (m+n)}^T}{\partial \eta^2} \\ \left(\frac{8}{a_2 b}\right) \frac{\partial^2 \{\Psi^{(2)}(r, \eta)\}_{1 \times (m+n)}^T}{\partial r \partial \eta} \end{bmatrix} \quad (44)$$

The buckling load N is obtained by solving the generalised eigenvalue equation defined by Eq. (36).

3. Results and discussions

The validity and accuracy of the proposed method are first verified through convergence and comparison studies. Buckling solutions are then presented for several selected rectangular plates of various aspect ratios and different combination of mixed edge support conditions.

Plates considered in this study are isotropic, elastic thin rectangular plates with Poisson's ratio $\nu = 0.3$. The buckling load N is expressed in terms of a non-dimensional buckling factor $\lambda = Nb^2 / (\pi^2 D)$. Symbols f , s and c are used to denote free, simply supported and clamped edge conditions, respectively.

3.1 Convergence and comparison studies

A square plate subjected to uniaxial in-plane load N and with mixed edge support conditions is

considered (see Fig. 3). The plate is partitioned into two subdomains along a line across the interface of the mix supports. It results in the plate with three simply supported edges on subdomain 1 and two free edges and one simply supported edge on subdomain 2, namely *sss-sff* plate.

Tables 1-3 presents buckling factors for the *sss-sff* square plate with the interface location of the two subdomains situating at $a_1/a = 0.25, 0.5$ and 0.75 , respectively. To examine the convergence of the buckling results, the degrees of the 2-D complete polynomial $p^{(1)}$ and $p^{(2)}$ are increased from 1 to 28. It is observed that the buckling factor λ decreases monotonically as the degrees of polynomial increases. When the polynomial degree on subdomain 2, $p^{(2)}$, is taken larger value than that on subdomain 1, $p^{(1)}$, the convergence rate of the buckling load factor λ is accelerated. For a fixed $p^{(1)}$, λ decreases as $p^{(2)}$ increases. This decrease is quite significant when $p^{(1)}$ is less than 10, and then the decrease rate tends to slow down. It is found that when $p^{(2)} = p^{(1)} + 3$, a lower value of λ can be achieved at a lower value of $p^{(1)}$. It is observed that the rate of convergence is greater when a_1/a takes a larger value.

The computation can continue for high value of $p^{(1)}$ before ill-matrix condition occurs. The buckling factor λ converges to an acceptable level as $p^{(1)}$ reaches to 15. Therefore all calculation in this paper is based on $p^{(1)} = 15$ and $p^{(2)} = p^{(1)} + 3 = 18$.

Table 1 Convergence study of buckling factor, $\lambda = Nb^2/\pi^2D$, for *sss-sff* square plate ($a_1/a = 0.25$)

Degree $p^{(1)}$	Polynomial degree on sub-domain 2: $p^{(2)}$					
	$p^{(2)} = p^{(1)}$	$p^{(2)} = p^{(1)} + 1$	$p^{(2)} = p^{(1)} + 2$	$p^{(2)} = p^{(1)} + 3$	$p^{(2)} = p^{(1)} + 4$	$p^{(2)} = p^{(1)} + 5$
1	3.1026	2.6222	2.4656	2.3940	2.3727	2.3648
2	2.5590	2.4154	2.3890	2.3716	2.3612	2.3557
3	2.4154	2.3824	2.3508	2.3301	2.3193	2.3151
4	2.3808	2.3453	2.3213	2.3088	2.3034	2.3003
5	2.3446	2.3201	2.3066	2.2997	2.2948	2.2909
6	2.3196	2.3052	2.2968	2.2903	2.2851	2.2818
7	2.3045	2.2955	2.2882	2.2825	2.2787	2.2763
8	2.2951	2.2876	2.2816	2.2774	2.2745	2.2724
9	2.2873	2.2810	2.2765	2.2732	2.2706	2.2686
10	2.2807	2.2760	2.2725	2.2697	2.2675	2.2659
11	2.2758	2.2722	2.2693	2.2670	2.2652	2.2637
12	2.2720	2.2690	2.2666	2.2646	2.2631	2.2618
13	2.2688	2.2663	2.2643	2.2627	2.2613	2.2603
14	2.2662	2.2641	2.2624	2.2610	2.2599	2.2589
15	2.2640	2.2623	2.2608	2.2596	2.2586	2.2578
16	2.2622	2.2607	2.2595	2.2584	2.2575	2.2568
17	2.2606	2.2594	2.2583	2.2574	2.2566	2.2559
18	2.2593	2.2582	2.2572	2.2564	2.2557	***
19	2.2581	2.2572	2.2563	2.2556	***	***
20	2.2571	2.2563	2.2555	***	***	***
21	2.2562	2.2555	***	***	***	***
22	***	***	***	***	***	***

***results can not be obtained due to ill-matrix condition

Table 2 Convergence study of buckling factor, $\lambda = Nb^2/\pi^2D$, for *sss-sff* square plate ($a_1/a = 0.5$)

Degree $p^{(1)}$	Polynomial degree on sub-domain 2: $p^{(2)}$					
	$p^{(2)} = p^{(1)}$	$p^{(2)} = p^{(1)} + 1$	$p^{(2)} = p^{(1)} + 2$	$p^{(2)} = p^{(1)} + 3$	$p^{(2)} = p^{(1)} + 4$	$p^{(2)} = p^{(1)} + 5$
1	4.3530	4.0694	3.9817	3.8884	3.8445	3.8285
2	3.8125	3.7488	3.7427	3.7351	3.7310	3.7295
3	3.7392	3.7219	3.7012	3.6908	3.6873	3.6860
4	3.7179	3.6911	3.6773	3.6720	3.6694	3.6675
5	3.6886	3.6741	3.6682	3.6647	3.6619	3.6603
6	3.6732	3.6664	3.6616	3.6577	3.6555	3.6544
7	3.6650	3.6590	3.6542	3.6514	3.6499	3.6488
8	3.6575	3.6523	3.6491	3.6472	3.6458	3.6447
9	3.6515	3.6480	3.6457	3.6439	3.6426	3.6418
10	3.6473	3.6447	3.6426	3.6411	3.6401	3.6393
11	3.6440	3.6417	3.6400	3.6388	3.6379	3.6372
12	3.6411	3.6393	3.6379	3.6369	3.6361	3.6355
13	3.6389	3.6374	3.6362	3.6354	3.6347	3.6342
14	3.6370	3.6358	3.6348	3.6340	3.6334	3.6330
15	3.6354	3.6344	3.6335	3.6329	3.6324	3.6320
16	3.6341	3.6332	3.6325	3.6319	3.6315	3.6311
17	3.6330	3.6322	3.6316	3.6311	3.6307	3.6303
18	3.6320	3.6313	3.6308	3.6304	3.6300	***
19	3.6312	3.6306	3.6301	3.6297	***	***
20	3.6304	3.6299	3.6295	***	***	***
21	3.6298	3.6293	***	***	***	***
22	3.6292	***	***	***	***	***
23	***	***	***	***	***	***

***results can not be obtained due to ill-matrix condition

Validity and accuracy of the present method can also be tested on a *ssc-sss* square plate. The plate is simply supported except part of an edge is clamped as shown in Fig. 4. The buckling factors λ are presented in Table 4 for the *ssc-sss* square plate with the interface of the two subdomains being placed at various locations. The buckling results obtained by Mizusawa and Leonard (1990) and Keer and Stahl (1972) are also shown in Table 4. It is observed that the buckling factors calculated using the proposed numerical model are in close agreement with the results from Mizusawa and Leonard (1990) and Keer and Stahl (1972).

3.2 Buckling factors for rectangular plates with mixed edge support conditions

Tables 5-8 present results for uniaxially loaded rectangular plates with different mixed boundary conditions. The plate aspect ratio a/b ranges from 0.5 to 3.0 at increment of 0.5. The location of the subdomain interface to the plate length ratio a_1/a is chosen to be 0, 0.25, 0.50, 0.75, and 1.0. The mixed edge conditions are arranged in such a way that the order of the support condition on the left portion of the edge is equal to or higher than the order on the right portion of the edge.

Table 3 Convergence study of buckling factor, $\lambda = Nb^2/\pi^2D$, for *sss-sff* square plate ($a_1/a = 0.75$)

Degree $p^{(1)}$	Polynomial degree on sub-domain 2: $p^{(2)}$					
	$p^{(2)} = p^{(1)}$	$p^{(2)} = p^{(1)} + 1$	$p^{(2)} = p^{(1)} + 2$	$p^{(2)} = p^{(1)} + 3$	$p^{(2)} = p^{(1)} + 4$	$p^{(2)} = p^{(1)} + 5$
1	4.3847	4.3729	4.3718	4.3671	4.3634	4.3613
2	4.0981	4.0974	4.0919	4.0914	4.0904	4.0898
3	3.9990	3.9987	3.9982	3.9981	3.9981	3.9980
4	3.9973	3.9966	3.9963	3.9961	3.9960	3.9959
5	3.9963	3.9961	3.9960	3.9959	3.9958	3.9958
6	3.9961	3.9959	3.9958	3.9958	3.9957	3.9957
7	3.9959	3.9957	3.9957	3.9956	3.9956	3.9956
8	3.9957	3.9956	3.9956	3.9955	3.9955	3.9955
9	3.9956	3.9955	3.9955	3.9955	3.9955	3.9954
10	3.9955	3.9955	3.9954	3.9954	3.9954	3.9954
11	3.9954	3.9954	3.9954	3.9953	3.9953	3.9953
12	3.9954	3.9953	3.9953	3.9953	3.9953	3.9953
13	3.9953	3.9953	3.9953	3.9953	3.9953	3.9952
14	3.9953	3.9953	3.9952	3.9952	3.9952	3.9952
15	3.9952	3.9952	3.9952	3.9952	3.9952	3.9952
16	3.9952	3.9952	3.9952	3.9952	3.9952	3.9952
17	3.9952	3.9952	3.9952	3.9951	3.9951	3.9951
18	3.9952	3.9951	3.9951	3.9951	3.9951	***
19	3.9951	3.9951	3.9951	3.9951	***	***
20	3.9951	3.9951	3.9951	***	***	***
21	3.9951	3.9951	***	***	***	***
22	3.9951	***	***	***	***	***
23	***	***	***	***	***	***

***results can not be obtained due to ill-matrix condition

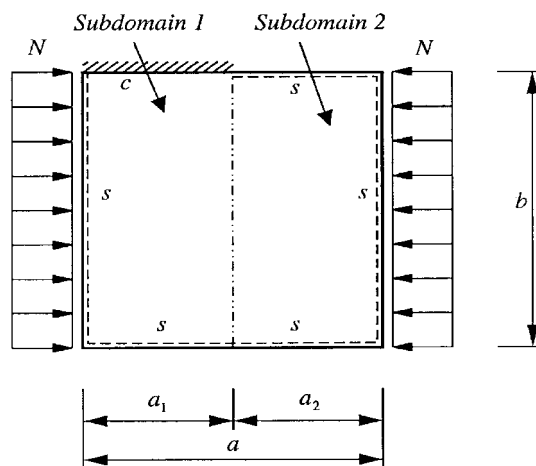
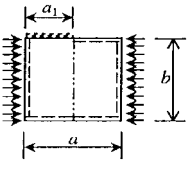
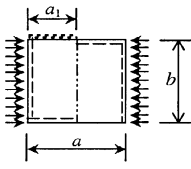
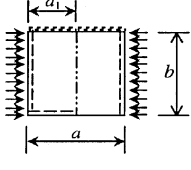
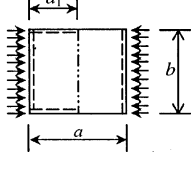


Fig. 4 A square plate subjected to uniaxial in-plane load and having mixed edge support conditions (*ssc-sss* plate)

Table 4 Comparison study of buckling factor, $\lambda = Nb^2/\pi^2D$, for *ssc-sss* square plate

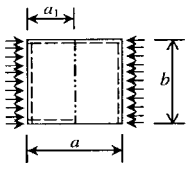
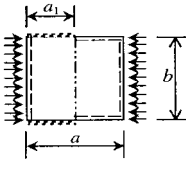
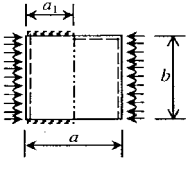
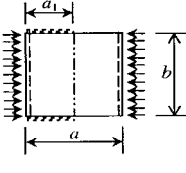
a_1/a	Present method	Mizusawa & Leonard (1990)	Keer & Stahl (1972)
0	4.0000	4.000	4.000
1/6	4.1813	4.209	4.149
1/5	4.2473	4.641	4.545
1/2	5.1252	5.198	5.090
2/3	5.5869	5.628	5.570
5/6	5.7313	5.736	5.731
1	5.7402	5.740	5.741

Table 5 Buckling factor, $\lambda = Nb^2/\pi^2D$, for rectangular plates with different mixed boundary conditions

Boundary Conditions	a/b	a_1/a				
		0	0.25	0.50	0.75	1.0
Case 1: <i>ssc-sss</i> plate	0.5	6.2500	6.4381	6.7201	6.8433	6.8531
	1.0	4.0000	4.3611	5.1252	5.6925	5.7402
	1.5	4.3403	4.4525	4.5948	5.2662	5.4312
	2.0	4.0000	4.2920	4.3713	5.1245	5.6056
	2.5	4.1344	4.1758	4.3627	4.7922	5.4232
	3.0	4.0000	4.1361	4.3025	4.5824	5.4312
Case 2: <i>ssc-sfs</i> plate	0.5	4.3558	6.0736	6.6755	6.8427	6.8531
	1.0	1.4016	2.8593	4.6339	5.6872	5.7402
	1.5	0.8578	1.7257	2.9722	5.1807	5.4312
	2.0	0.6681	1.1984	2.0119	4.6115	5.6056
	2.5	0.5806	0.9342	1.4971	3.7170	5.4232
	3.0	0.5331	0.7853	1.1947	2.9692	5.4312
Case 3: <i>ssc-sfc</i> plate	0.5	4.4633	6.3853	6.8035	6.8523	6.8531
	1.0	1.6525	3.2585	5.1253	5.7351	5.7402
	1.5	1.2912	2.0709	3.2923	5.3546	5.4312
	2.0	1.3360	1.6171	2.3279	5.0137	5.6056
	2.5	1.3852	1.4700	1.8525	4.0864	5.4232
	3.0	1.2912	1.4468	1.6125	3.2970	5.4312
Case 4: <i>sss-sff</i> plate	0.5	3.8926	5.6762	6.1828	6.2489	6.2500
	1.0	0.9523	2.2596	3.6329	3.9952	4.0000
	1.5	0.4168	1.2026	2.4025	4.2576	4.3403
	2.0	0.2322	0.7163	1.4893	3.7327	4.0000
	2.5	0.1477	0.4708	1.0005	3.0736	4.1344
	3.0	0.1022	0.3323	0.7152	2.3890	4.0000

----- : Simple support, - - - - - : Clamped support, ——— : Free

Table 6 Buckling factor, $\lambda = Nb^2/\pi^2D$, for rectangular plates with different mixed boundary conditions

Boundary Conditions	a/b	a_1/a				
		0	0.25	0.50	0.75	1.0
Case 5: <i>sss-sfs</i> plate	0.5	4.3558	5.9250	6.2159	6.2494	6.2500
	1.0	1.4016	2.7478	3.8133	3.9976	4.0000
	1.5	0.8578	1.7075	2.9093	4.3001	4.3403
	2.0	0.6681	1.1951	1.9908	3.8847	4.0000
	2.5	0.5806	0.9330	1.4879	3.4955	4.1344
	3.0	0.5331	0.7845	1.1900	2.8834	4.0000
Case 6: <i>scc-sss</i> plate	0.5	6.2500	6.6452	7.3243	7.6630	7.6913
	1.0	4.0000	4.6759	5.9870	7.4715	7.6913
	1.5	4.3403	4.4710	4.7764	6.4312	7.1159
	2.0	4.0000	4.3697	4.4679	5.7359	6.9716
	2.5	4.1344	4.1921	4.4282	5.1707	6.9989
	3.0	4.0000	4.1529	4.3654	4.7951	7.0552
Case 7: <i>scc-sfs</i> plate	0.5	4.3558	6.4351	7.3122	7.6610	7.6913
	1.0	1.4016	3.1312	5.3567	7.4632	7.6913
	1.5	0.8578	1.7956	3.1711	6.3378	7.1159
	2.0	0.6681	1.2277	2.1070	5.2199	6.9716
	2.5	0.5806	0.9504	1.5487	4.0632	6.9989
	3.0	0.5331	0.7953	1.2260	3.1796	7.0552
Case 8: <i>scc-sff</i> plate	0.5	3.8926	6.2667	7.3015	7.6591	7.6913
	1.0	0.9523	2.6475	4.9928	7.4559	7.6913
	1.5	0.4168	1.3144	2.6870	6.2522	7.1159
	2.0	0.2322	0.7631	1.6222	4.8895	6.9716
	2.5	0.1477	0.4964	1.0746	3.6075	6.9989
	3.0	0.1022	0.3484	0.7613	2.6934	7.0552

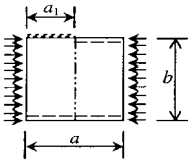
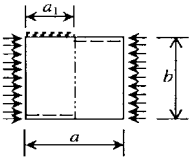
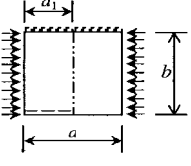
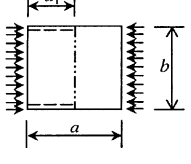
----- : Simple support, : Clamped support, ——— : Free

It is observed that the buckling factor λ increases as the subdomain length ratio a_1/a increases for all considered cases. It is because the constraints on the mixed edges become stronger while the subdomain interface moves from the left to the right side. The rate of increase in buckling factors is significant when a_1/a is less than 0.75.

4. Conclusions

This paper presents a new numerical model for buckling of rectangular plates with mixed boundary conditions. A plate is decomposed into two subdomains and the C^1 continuity conditions on the entire interface of the two subdomains are enforced. The automated Ritz method has been

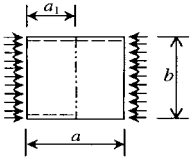
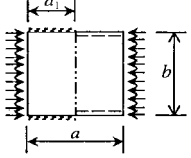
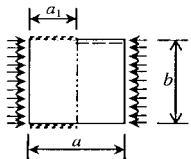
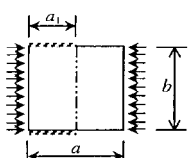
Table 7 Buckling factor, $\lambda = Nb^2/\pi^2D$, for rectangular plates with different mixed boundary conditions

Boundary Conditions	a/b	a_1/a				
		0	0.25	0.50	0.75	1.0
Case 9: <i>fsc-fss</i> plate	0.5	1.5820	1.7117	1.7546	1.8990	2.0337
	1.0	2.0429	2.2937	2.3020	2.4731	3.0611
	1.5	2.2563	2.3119	2.3451	2.3782	2.9528
	2.0	2.2607	2.3089	2.3333	2.3545	3.0629
	2.5	2.3041	2.3102	2.3180	2.3521	3.0535
	3.0	2.3048	2.3101	2.3112	2.3503	3.0636
	Case 10: <i>fsc-ffs</i> plate	0.5	---	0.8721	1.2645	1.7594
	1.0	---	0.6474	0.9249	1.7091	3.0611
	1.5	---	0.5351	0.6829	1.2231	2.9528
	2.0	---	0.4830	0.5722	0.9461	3.0629
	2.5	---	0.4571	0.5158	0.7849	3.0535
	3.0	---	0.4429	0.4838	0.6846	3.0636
	Case 11: <i>fsc-ffc</i> plate	0.5	0.4622	1.0399	1.4482	1.8806
	1.0	0.6125	0.9575	1.1874	1.9857	3.0611
	1.5	0.7766	0.9560	0.9985	1.4783	2.9528
	2.0	0.8323	0.9429	0.9588	1.2079	3.0629
	2.5	0.8169	0.9063	0.9568	1.0688	3.0535
	3.0	0.8369	0.8828	0.9432	0.9997	3.0636
	Case 12: <i>fss-fff</i> plate	0.5	---	0.5101	0.9091	1.3822
	1.0	---	0.2490	0.5064	1.2174	2.0429
	1.5	---	0.1350	0.2776	0.7904	2.2563
	2.0	---	0.0824	0.1712	0.5297	2.2607
	2.5	---	0.0551	0.1157	0.3763	2.3041
	3.0	---	0.0393	0.0833	0.2801	2.3048

--- results can not be obtained due to the plate being externally unstable
 ----- : Simple support,  : Clamped support,  : Free

employed to derive the governing eigenvalue equations. The correctness and accuracy of the proposed method have been verified through convergence and comparison studies. Buckling results have been presented for rectangular plates of different aspect ratios and having various combination of mixed support conditions. These results are very useful for engineers to design plates with mixed boundary conditions and for researchers to check their numerical models. It is noted that the present method is readily to be applied to deal with buckling of rectangular plates subjected to bi-axial in-plane load and vibration of rectangular plates. The study for plates with multiple subdomains is being carried out by the authors.

Table 8 Buckling factor, $\lambda = Nb^2/\pi^2D$, for rectangular plates with different mixed boundary conditions

Boundary Conditions	a/b	a_1/a				
		0	0.25	0.50	0.75	1.0
Case 13: <i>fss-ffs</i> plate	0.5	---	0.8444	1.1711	1.4771	1.5820
	1.0	---	0.6344	0.8958	1.5432	2.0429
	1.5	---	0.5310	0.6775	1.1866	2.2563
	2.0	---	0.4817	0.5705	0.9318	2.2607
	2.5	---	0.4565	0.5149	0.7782	2.3041
	3.0	---	0.4427	0.4833	0.6809	2.3048
Case 14: <i>fcc-fss</i> plate	0.5	1.5820	1.7973	1.9197	2.2875	2.6645
	1.0	2.0429	2.3540	2.3653	2.6419	3.6564
	1.5	2.2563	2.3251	2.3674	2.4334	3.8324
	2.0	2.2607	2.3118	2.3464	2.3776	3.8549
	2.5	2.3041	2.3103	2.3228	2.3706	3.8771
	3.0	2.3048	2.3102	2.3126	2.3689	3.8775
Case 15: <i>fcc-ffs</i> plate	0.5	---	0.9784	1.5047	2.2241	2.6645
	1.0	---	0.6813	0.9991	1.9916	3.6564
	1.5	---	0.5449	0.7058	1.3466	3.8324
	2.0	---	0.4867	0.5825	1.0096	3.8549
	2.5	---	0.4588	0.5212	0.8213	3.8771
	3.0	---	0.4439	0.4870	0.7072	3.8775
Case 16: <i>fcc-fff</i> plate	0.5	---	0.6378	1.2502	2.1674	2.6645
	1.0	---	0.2921	0.6158	1.6695	3.6564
	1.5	---	0.1506	0.3157	0.9739	3.8324
	2.0	---	0.0895	0.1896	0.6255	3.8549
	2.5	---	0.0590	0.1262	0.43307	3.8771
	3.0	---	0.0417	0.0899	0.3169	3.8775

--- results can not be obtained due to the plate being externally unstable.

----- : Simple support,  : Clamped support,  : Free

Acknowledgements

The authors would like to thank the Australian Research Council for partial support of this work through an ARC Small Grant.

References

Bartlett, C.C. (1963), "The vibration and buckling of a circular plate clamped on part of its boundary and simply supported on the remainder", *Quart. J. Mech. & Appl. Math.* **16**, 431-440.

- Bulson, P.S. (1970), *The Stability of Flat Plates*. Chatto and Windus, London, U.K.
- Column Research Committee of Japan. (1971), *Handbook of Structural Stability*. Corona, Tokyo, Japan.
- Hamada, H., Inoue, Y. and Hashimoto, H. (1967), "Buckling of simply supported but partially clamped rectangular plates uniformly compressed in one direction", *Bulletin of Japan Society of Mechanical Engineers* **10**, 35-40.
- Karamanlidis, D. and Prakash, V. (1989), "Buckling and vibrations of shear-flexible orthotropic plates subjected to mixed boundary conditions", *Thin-Walled Structures*, **8**, 273-293.
- Keer, L.M. and Stahl, B. (1972), "Eigenvalue problems of rectangular plates with mixed edge conditions", *J. Appl. Mech.*, **39**, 513-520.
- Liew, K.M., Wang, C.M., Xiang, Y. and Kitipornchai, S. (1998), *Vibration of Mindlin Plates -- Programming the p-Version Ritz Method*. Elsevier Science Ltd, Amsterdam, The Netherlands.
- Lim, C.W. and Liew, K.M. (1993), "Effects of boundary constraints and thickness variations on the vibratory response of rectangular plates", *Thin-Walled Structures*, **17**, 133-159.
- Mizusawa, T. and Leonard, J.W. (1990), "Vibration and buckling of plates with mixed boundary conditions", *Eng. Struct.*, **12**, 285-290.
- Reddy, J.N. and Phan, N.D. (1985), "Stability and vibration of isotropic, orthotropic and laminated plates according to a higher-order shear deformation theory", *J. Sound Vib.*, **98**, 157-170.
- Sakiyama, T. and Matsuda, H. (1987), "Elastic buckling of rectangular Mindlin plates with mixed boundary conditions", *Computers and Structures*, **25**, 801-808.
- Xiang, Y., Wang, C.M. and Kitipornchai, S. (1995), "Shear buckling of skew Mindlin plates", *AIAA J.*, **33**, 377-378.
- Xiang, Y., Wang, C.M. and Kitipornchai, S. (1996), "Optimal location of point supports in plates for maximum fundamental frequency", *Structural Optimization*, **11**, 171-177.